A Three Phase Active Rectifier Control Mechanism using d-q Components of Phase Currents

Tanvir Alam Shifat
School of Electrical Engineering and
Computer Science
Oregon State University
Corvallis, OR, USA
shifatt@oregonstate.edu

I. INTRODUCTION

Power conversion is a crucial yet quite frequently done operation in electrical systems. Based on the necessity of a particular electrical component, power needs to be converted from DC to AC or AC to DC in a short period of time with high accuracy and efficiency. This process is called "rectification," and hence, the device that performs this operation is called a "rectifier" [1]. As most electrical transmission systems use AC power to deliver power to households and most household appliances require DC power to operate, we need rectifiers to convert the grid's high voltage AC power to low voltage DC power. Besides, rectifiers are widely used in the detection and amplitude modulation of radio signals, supplying the polarized voltage for welding, controlling traction motors in railways, switched-mode power supplies, etc. [1-2]. Using only the switches does the essential operation of converting AC into DC; however, that DC output is often affected by rising and falling pulsations known as ripples. An electronic filter is used to smooth the rectifier output, and most of the time, it is a capacitor connected in parallel with the load.

Depending on the bus voltage requirement, rectifiers can be of two types: half-bridge and full-bridge. Full-bridge rectifiers are used to take advantage of the entire AC power over a half-bridge, which utilizes only half of the total power. With the advancement in power electronic components, different switches can be used to form the full bridge in a rectifier circuit. The most basic full-bridge rectifier is built using diodes. However, diodes are passive, and they cannot be controlled by external turn ON and turn OFF signals. While the diode-based rectifiers are simple in design and easy to control, PWM-controlled active rectifiers drastically reduce the input current harmonics and enable bidirectional power flow. These rectifiers are also referred to as synchronous rectifiers [2]. Active rectifiers are also useful in systems that require a sophisticated control mechanism before delivering the power to the load. To enhance the control mechanism, several active switches are used in a rectifier circuit, such as a thyristor, metal oxide semiconductor field-effect transistor (MOSFET), insulated gate bipolar transistor (IGBT), etc. Active rectification is widely adopted in electric locomotives, DC traction motors, power factor correction circuits, photovoltaics, etc. [2-3].

One major characteristic that makes the active rectifiers different is their control strategy. Synchronous switches in these rectifiers require an external control mechanism to turn ON and OFF at a particular interval. The amount of time a switch remains ON is called "duty." Diving this time by the total period gives us the "duty ratio," a commonly used term in switching devices [3]. Control of the rectifier is dependent mainly on the AC source and load connected to it. The principal goal of the rectifier is to maintain a constant DC bus voltage across the load. Almost every control technique comprises comparing the DC link voltage to the reference voltage and modifying control parameters to reduce the error between output and the reference voltage.

In literature, several physics-based and mathematical models are studied. For example, Qiang *et al.* proposed a double voltage loop feedback controller for PWM rectifiers [4]. Ohnuki *et al.* used a control algorithm without directly measuring the AC side and DC side voltages rather than by estimation [5]. Fekik *et al.* used a backstepping algorithm for power control in rectifiers [6]. Bouafia *et al.* proposed two different control strategies named space-vector modulation (SVM) and fuzzy logic-based switching state for three-phase active rectifier control [7-8]. Several other electrical measurements are taken into consideration for the control of active rectifiers. For example, Bing *et al.* used a single DC current sensor measurements [9], and Cho *et al.* used a virtual-flux-based fast dynamic response for predictive direct power control [10]. While these approaches obtain the goal set for the specific task, their mathematical representation is complicated and requires complete modification to deploy in a different system with a different set of requirements. Given the wide range of diverse applications in power electronics converters, we believe a robust control technique is necessary for active rectifiers that can be implemented for a range of DC bus voltage requirements.

This project focuses on the high-power pulsed load application with a three-phase AC source connected to it. Broader application of this active rectifier system is high power electric vehicle (EV) charging, hybrid energy storage systems, etc. Notably, this system can be implemented where a large amount of power is required for a very short period of time. We propose an IGBT-based active rectifier with PWM signals controlled by the d-q components of the phase currents. Several existing technologies, such as space vector modulation, virtual flux control, etc., require a set of vector representations and mathematical interpretation of the entire generator-rectifier system. These approaches are mathematically sound yet work best for some system-specific applications and require robust physical modeling. Our proposed method uses an *abc-dq* transformation of phase currents which is fed into the current controller, and the rectifier's output voltage is used with the reference voltage as an input to the voltage controller. Both the controllers are necessarily PI-based linear controller that quickly simulates the system and preserves both the current and voltage characteristics of the generator-rectifier system. Therefore, we have a reliable and straightforward rectifier control, having both the generator (source) and the output DC voltage (load) characteristics present.

Submitted as a partial fulfillment for ECE599 Project in Spring 2022.

II. Proposed Converter and System

A. Rectifier and Control

A three-phase active rectifier is proposed based on IGBT switches and the SPWM modulation technique. We have used a cascaded PI controller to control the rectifier's output (DC bus) voltage by taking into account both the d-axis and q-axis I-V characteristics of the three-phase source signal. Unlike regular control algorithms, modeling with d-q components is advantageous because controller gains are able to modulate bus voltage for a larger margin. Thus, we can produce different DC voltage ranges by keeping the same gains at the rectifier output. Park's transformation allows us to use a frame of reference on the rotor in which I_a, I_b, and I_c are co-planar three-phase quantities at an angle of 120° each other [11]. This relation is mathematically expressed in (1) and a pictorial illustration is shown in Fig. 1. We have used MATLAB/Simulink built-in block to obtain equivalent d-q current and voltage components. A more detailed explanation of orthogonal two-dimensional representation of three-phase signals can be found in [12-13].

$$\begin{bmatrix} i_q \\ i_d \end{bmatrix} = \frac{2}{3}\begin{bmatrix} \cos\theta & \cos(\theta-120) & \cos(\theta+120) \\ \sin\theta & \sin(\theta-120) & \sin(\theta+120) \end{bmatrix}\begin{bmatrix} i_a \\ i_b \\ i_c \end{bmatrix} \quad (1)$$

Later, $I_{d,ref}$ is generated by considering the error between reference DC voltage and generated DC voltage at the rectifier end. This relationship is expressed in (2). Finally, two controlled d-q components of the voltage are calculated using equations (3) and (4).

$$I_{d,ref} = K_{p1}(V_{ref} - V_{dc}) + K_{i1}\int (V_{ref} - V_{dc})dt \quad (2)$$

$$V_{d,cont} = K_{p2}(I_{d,ref} - I_d) + K_{i2}\int (I_{d,ref} - I_d)dt \quad (3)$$

$$V_{q,cont} = K_{p3}(I_{q,ref} - I_q) + K_{i3}\int (I_{q,ref} - I_q)dt \quad (4)$$

From the $V_{d,cont}$ and $V_{q,cont}$ signals, an inverse Park transformation is performed to obtain the respective three phase AC signals [14]. Matrix representation of this transformation is shown in (5).

$$\begin{bmatrix} V_a \\ V_b \\ V_c \end{bmatrix} = \begin{bmatrix} \cos\theta & \sin\theta \\ \cos(\theta-120) & \sin(\theta-120) \\ \cos(\theta+120) & \sin(\theta+120) \end{bmatrix}\begin{bmatrix} V_q \\ V_d \end{bmatrix} \quad (5)$$

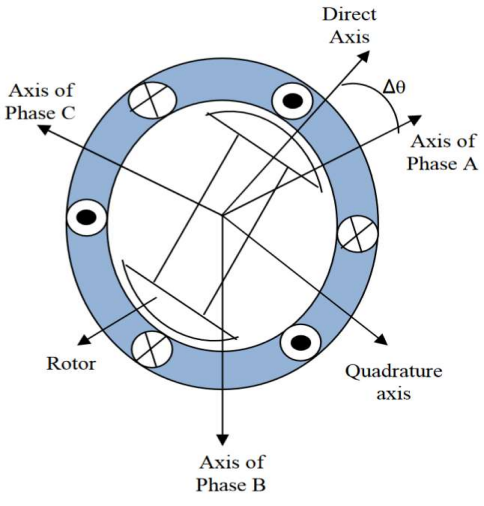

Fig. 1: PMSG representation illustrating d-q frame [12].

Signal obtained through inverse Park's transformation (reference signals) are compared with a high-frequency triangular carrier waveform to generate the desired PWM signals which are later fed into the IGBT switches. Three PWM signals are generated from V_{abc} reference signals and other three are generated by taking the complementation of previous ones.

B. System Integration

A supercapacitor (SC) module is designed to use as a load to the rectifier system. SC is a promising energy storage device that can charge and discharge rapidly with high energy density. It is being highly acknowledged and unanimously envisaged as a promising energy storage system (ESS) technology. Compared to conventional capacitors, SC has a much higher capacitance, enabling high energy density. Particularly, delivering a high amount of power in a short period, even in extreme temperatures, has made them popular in pulsed power applications. As mentioned earlier, supercapacitors are well known for their high energy density and can produce a large amount of pulsed power in a short period of time. This design of SC module is expected to deliver 1 kW in every 5 seconds of a 15 seconds of period. A buck converter is placed within the SC module which acts as a charging circuit.

In case of source, we have used a three-phase source coupled with the rectifier with an LR filter in between. This filter is used to get rid of low frequency current harmonics when the source is connected to a load. Capacitive load created significant number of ripples at the input current end and a filter is required to suppress the ripple effect. Cut-off frequency for the filter is as follow:

$$f_{cutoff} = \frac{1}{2\pi(\frac{L}{R})} = \frac{R}{2\pi L} \quad (6)$$

For the filter design we have selected L = 1 mH and R = 100 mΩ making the time constant, τ = 10 ms and cut-off frequency $f_{cutoff} = 15.92$ Hz. Selecting these parameters are design choice and can be modified based on design requirement. An illustration of the proposed system is presented in Fig. 2.

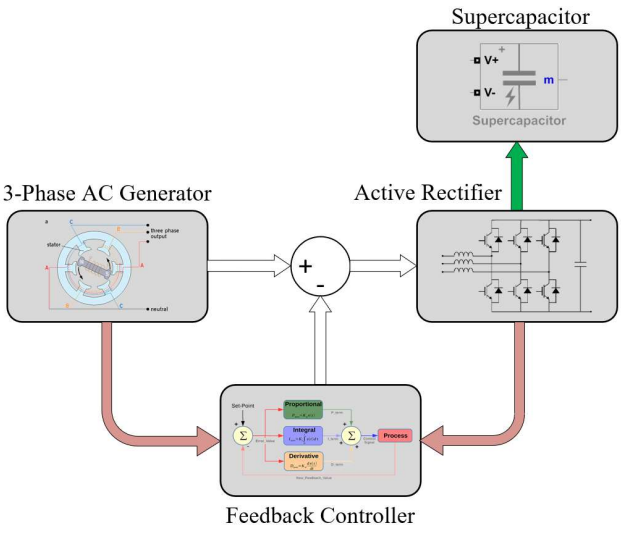

Fig. 2: Proposed system architecture

III. Example Design and Simulation Results

The proposed system is built on a *simpower* domain of MATLAB/Simulink using appropriate blocks and connections. A three-phase I-V measurement block is used to measure the source current and voltages. Several series RLC branch is used to create the necessary resistor, inductor, and capacitor elements. IGBT/Diode is used as the active switch to build full-bridge active rectifier. A scope is used to visualize all the necessary signals for the entire simulation period.

Different controller gains are directly put into the built-in PID controller block. A list of controller gains used in this model is presented in TABLE I. For the SC module model, we have used the built-in supercapacitor model, which allows us to modify the number of cells in series, Ns, the number of cells in parallel, Np, and each cell rated voltage and capacitance. SC module parameters are presented in TABLE II.

Different signals obtained from the system are presented in Fig. 2-5. Fig. 2 (lower right) represents the trend of V_{REF} and V_{DC}. It can be observed that V_{DC} immediately follows the required V_{REF} at different levels. As mentioned earlier, in this project we focus on different ranges of DC bus voltages instead of one. This can be seen in Fig. 3 also. As a different bus voltage is required by the V_{REF}, the I_d commands V_d and V_q to produce required amount of PWM signals which are later fed into IGBT switches. A more scaled in version of Fig. 3 is presented in Fig. 4 to better observe signal trends. We can see some current ripples in the input currents as well as some voltage ripple in the output voltage. However, compared to the level of voltage in this converter, these ripples are ignorable.

V_{DC} is then fed into SC module to produce the required pulsed power output. Trends in SC output voltage and current with respective SOC levels are shown in Fig. 5. And, the

TABLE I: Controller gains

Gain	*Value*	*Gain*	*Value*
K_{p1}	0.2	K_{i1}	100
K_{p2}	0.023	K_{i2}	20
K_{p3}	0.023	K_{i3}	20

TABLE II: Supercapacitor model

Parameter	*Value*	*Parameter*	*Value*
Cell voltage	2.7 V	$E_{rated,cell}$	10.935 kJ
Cell capacitance	3000 F	Module voltage	270 V
N_s	100	Module capacitance	60 F
N_p	2	$E_{rated,module}$	2.187 MJ
N_{cell}	200	ESR	2.1 mΩ

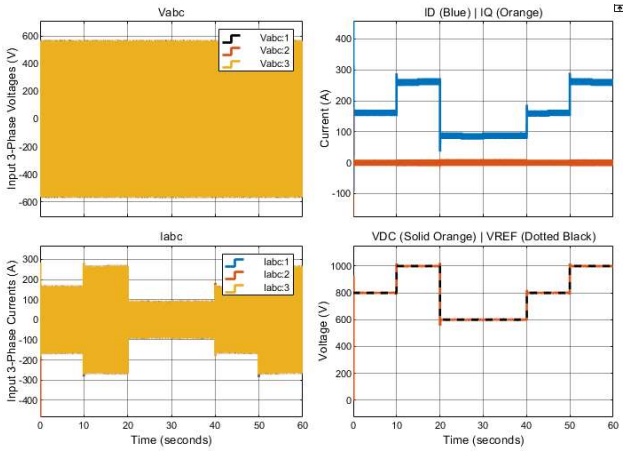

Fig. 3: Rectifier output with source and control signals.

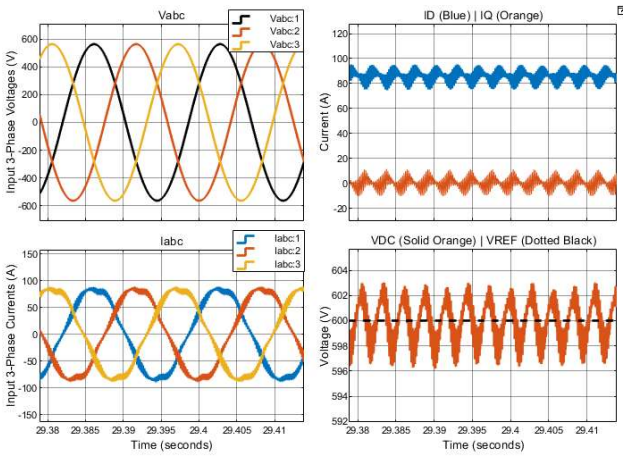

Fig. 4: Rectifier output with source and control signals (Zoom-in).

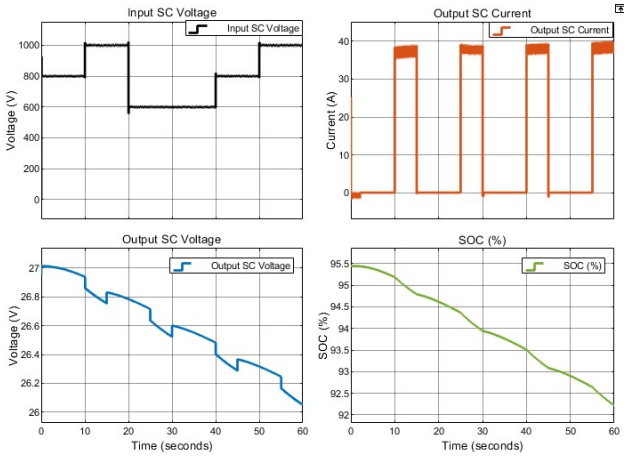

Fig. 5: SC module I-V and SOC trend.

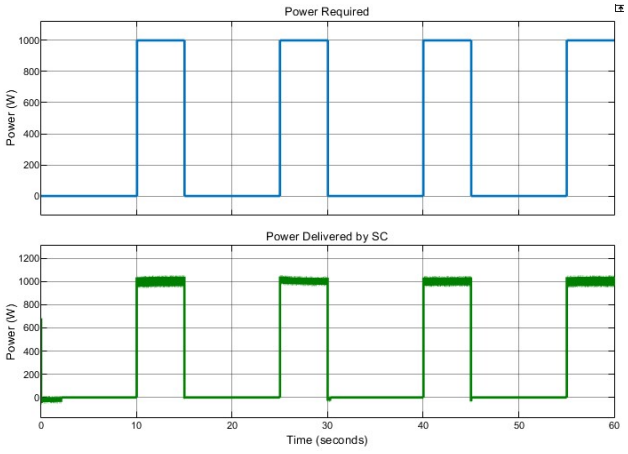

Fig. 6: Expected and delivered pulsed power output.

reference power and delivered power are shown in Fig. 6. SC was able to produce 1 kW of power for every 5 seconds in a 15 second period. In the other 10 seconds the power is commanded to be zero and considered as the charging state of the SC module. The SOC drops from 95.5% to 92% during the 60 seconds of runtime. In this case, some ripples in the SC current are observed and due to this, the pulsed powers also exhibit some ripples. This ripple is not related to the previously seen ripple in rectifier. This is due to SC module's internal equivalent series resistance (ESR) and charging control circuit parameter optimization. However, this ripple is not too large to be considered as a flaw in the system.

IV. Result Analysis and Discussion

This model is properly working as per the design requirement and proposed model. Rectifier controller is able to hold the voltage at different levels of reference voltages with a very low amount of error. Different voltages and current at different time intervals are presented in TABLE III.

Time intervals are divided into five sections when the reference voltage (V_{REF}) command is varied. We can see that based on the V_{REF}, I_d and I_{abc} changes and hence the V_{DC} also follows the V_{REF} trend.

Finally, the SC module has successfully delivered the power required while connected to the generator-rectifier system. Pulsed power output is produced in the interval of 10-15, 25-30, 40-45, and 55-60 seconds. In this case, the SC module voltage V_{SC} goes down, but the module current, I_{SC}, keeps increasing with the time to keep up with the required power. This indicates that this system can be used for an application where a low voltage high current is necessary by connecting fewer SC cells in series and more in parallel.

Overall, the proposed generator-rectifier-supercapacitor system has been synced quite well, providing the desired output. However, there are some scopes to improve the source and load ends system.

In the case of source, we have used a three-phase source to replicate the behavior of a permanent magnet synchronous generator (PMSG). The original PMSG model requires an external control algorithm to modulate the filed voltage for three-phase power generation. This causes the entire system to reach in steady state after about 30 seconds. Since our entire simulation is set to run for 60 seconds, it is not wise to compromise half of the runtime for the PMSG model to come into steady-state condition. Also, in real-life applications, we do not expect the generator would start and stop at a certain interval. We expect a generator to run uninterruptedly. Hence, instead of compromising the initial biasing time for the PMSG model, we used an ideal three-phase source to produce the required AC power. However, an LR filter was good enough to suppress the input current ripple in this case. When implementing the PMSG model, we will require a higher order filter, such as an LCL filter, to reduce current harmonics.

TABLE III: Rectifier output analysis

Parameter	***Time periods (seconds)***				
	0-10	*10-20*	*20-40*	*40-50*	*50-60*
$V_{abc,rms}$ (V)	400	400	400	400	400
$I_{abc,rms}$ (A)	160	260	90	160	260
V_{REF} (V)	800	1000	600	800	1000
V_{DC} (V)	800	1000	600	800	1000
$V_{DC,ripple}$ (%)	±1.05	±1.15	±1	±1.05	±1.15
I_d (A)	160	260	90	160	260
I_q (A)	0	0	0	0	0

TABLE IV: Pulsed power output analysis

Parameter	***Pulsed power periods (seconds)***			
	10-15	*25-30*	*40-45*	*55-60*
V_{DC} (V)	800	1000	600	800
P_{REF} (W)	1000	1000	1000	1000
V_{SC} (V)	26.85	26.7	26.5	26.2
I_{SC} (A)	37.24	37.45	37.74	38.17
P_{SC} (W)	1000	1000	1000	1000
SOC (%)	95	94	93.5	92.5

The SC module is small compared to the DC bus voltage in terms of load. A larger SC module is required to make this model realistic. Also, the SC module charging circuit can be combined with the active rectifier model to supply a desired DC voltage at the SC end.

V. Conclusion

An IGBT-based active rectifier with connected three-phase source and supercapacitor load is proposed. A simple PI controller is designed by taking d-q current components as input and voltage components as the controlled variable. Park's transformation is done to find orthogonal two-dimensional parameters of the three-phase current signals. Using the d-q current components, a set of controlled d-q voltage components are produced and fed into PWM generation block through an inverse Park's transformation. The rectifier converter is connected to a system where the generator is input, and a supercapacitor module acts as a load. The rectifier controller can keep up with the variable reference voltage commanded at the DC bus. Also, the SC module was able to deliver the required power while being connected to the active rectifier. Different quantitative analysis including different current and voltage magnitudes at different reference voltage level are presented. Output voltage ripple at the DC bus and SC current ripple at the load end are approximated. Compared to existing control techniques which require a solid mathematical representation of the system, this control approach is simple yet robust.

In the future, this work can be extended to control a bigger size of SC module with more cells in series/parallel combinations. Also, a higher-order filter can be designed at the input end to further suppress the input current ripple while being connected to a capacitive load.

REFERENCES

[1] Wikipedia contributors. (2022, April 15). Rectifier. In *Wikipedia, The Free Encyclopedia*. Retrieved 08:51, June 5, 2022, from https://en.wikipedia.org/w/index.php?title=Rectifier&oldid=1082853614

[2] M. H. Rashid, "Three-Phase Controlled Rectifiers," *Power Electronics Handbook*, pp. 233–273, 2018, doi: 10.1016/b978-0-12-811407-0.00009-x.

[3] "PWM Current Source Rectifiers," *High-Power Converters and AC Drives*, pp. 257–286, Dec. 2016, doi: 10.1002/9781119156079.ch11.

[4] Qiang, Wen, et al. "Simulation study of three-phase PWM rectifier with square of the voltage double closed loop control." *IOP Conference Series: Materials Science and Engineering*. Vol. 199. No. 1. IOP Publishing, 2017.

[5] T. Ohnuki, O. Miyashita, P. Lataire and G. Maggetto, "Control of a three-phase PWM rectifier using estimated AC-side and DC-side voltages," in IEEE Transactions on Power Electronics, vol. 14, no. 2, pp. 222-226, March 1999, doi: 10.1109/63.750174.

[6] Fekik, Arezki, et al. "Direct power control of three-phase PWM-rectifier with backstepping control." *Backstepping Control of Nonlinear Dynamical Systems*. Academic Press, 2021. 215-234.

[7] A. Bouafia, J. Gaubert and F. Krim, "Predictive Direct Power Control of Three-Phase Pulsewidth Modulation (PWM) Rectifier Using Space-Vector Modulation (SVM)," *IEEE Transactions on Power Electronics*, vol. 25, no. 1, pp. 228-236, Jan. 2010, doi: 10.1109/TPEL.2009.2028731.

[8] A. Bouafia, F. Krim and J. Gaubert, "Fuzzy-Logic-Based Switching State Selection for Direct Power Control of Three-Phase PWM Rectifier," I*EEE Transactions on Industrial Electronics*, vol. 56, no. 6, pp. 1984-1992, June 2009, doi: 10.1109/TIE.2009.2014746.

[9] Z. Bing, X. Du and J. Sun, "Control of Three-Phase PWM Rectifiers Using A Single DC Current Sensor," *IEEE Transactions on Power Electronics*, vol. 26, no. 6, pp. 1800-1808, June 2011, doi: 10.1109/TPEL.2010.2070809.

[10] Y. Cho and K. Lee, "Virtual-Flux-Based Predictive Direct Power Control of Three-Phase PWM Rectifiers With Fast Dynamic Response," *IEEE Transactions on Power Electronics*, vol. 31, no. 4, pp. 3348-3359, April 2016, doi: 10.1109/TPEL.2015.2453129.

[11] Z. Zeng, W. Zheng, R. Zhao, C. Zhu and Q. Yuan, "The Comprehensive Design and Optimization of the Post-Fault Grid-Connected Three-Phase PWM Rectifier," *IEEE Transactions on Industrial Electronics*, vol. 63, no. 3, pp. 1629-1642, March 2016, doi: 10.1109/TIE.2015.2494854.

[12] F. V. Lopes, D. Fernandes and W. L. A. Neves, "A Traveling-Wave Detection Method Based on Park's Transformation for Fault Locators," in IEEE Transactions on Power Delivery, vol. 28, no. 3, pp. 1626-1634, July 2013, doi: 10.1109/TPWRD.2013.2260182.

[13] K. Andanapalli and B. R. K. Varma, "Park's transformation based symmetrical fault detection during power swing," 2014 Eighteenth National Power Systems Conference (NPSC), 2014, pp. 1-5, doi: 10.1109/NPSC.2014.7103817.

[14] Zhou, Z., et al. "Design and analysis of a feedforward control scheme for a three-phase voltage source pulse width modulation rectifier using sensorless load current signal." *IET Power Electronics* 2.4 (2009): 421-430.

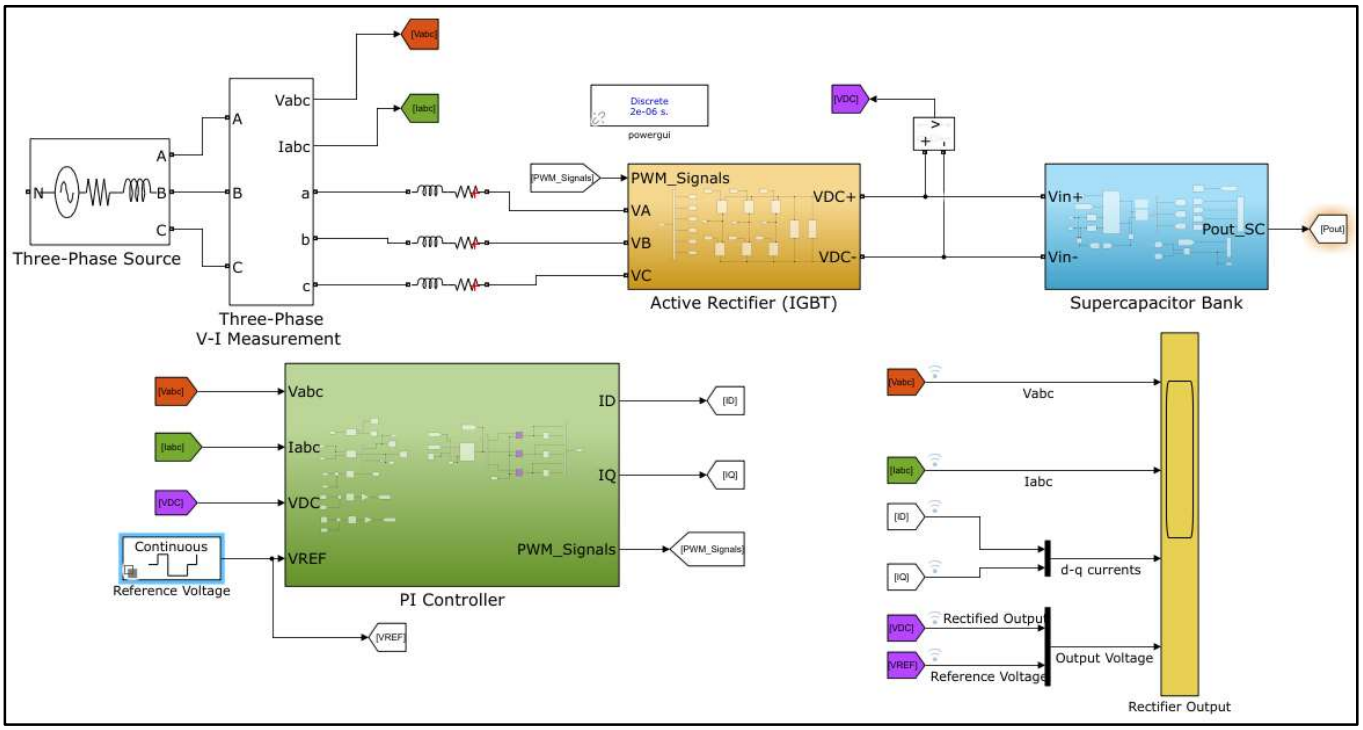

Figure: MATLAB/Simulink block diagram of the entire system.

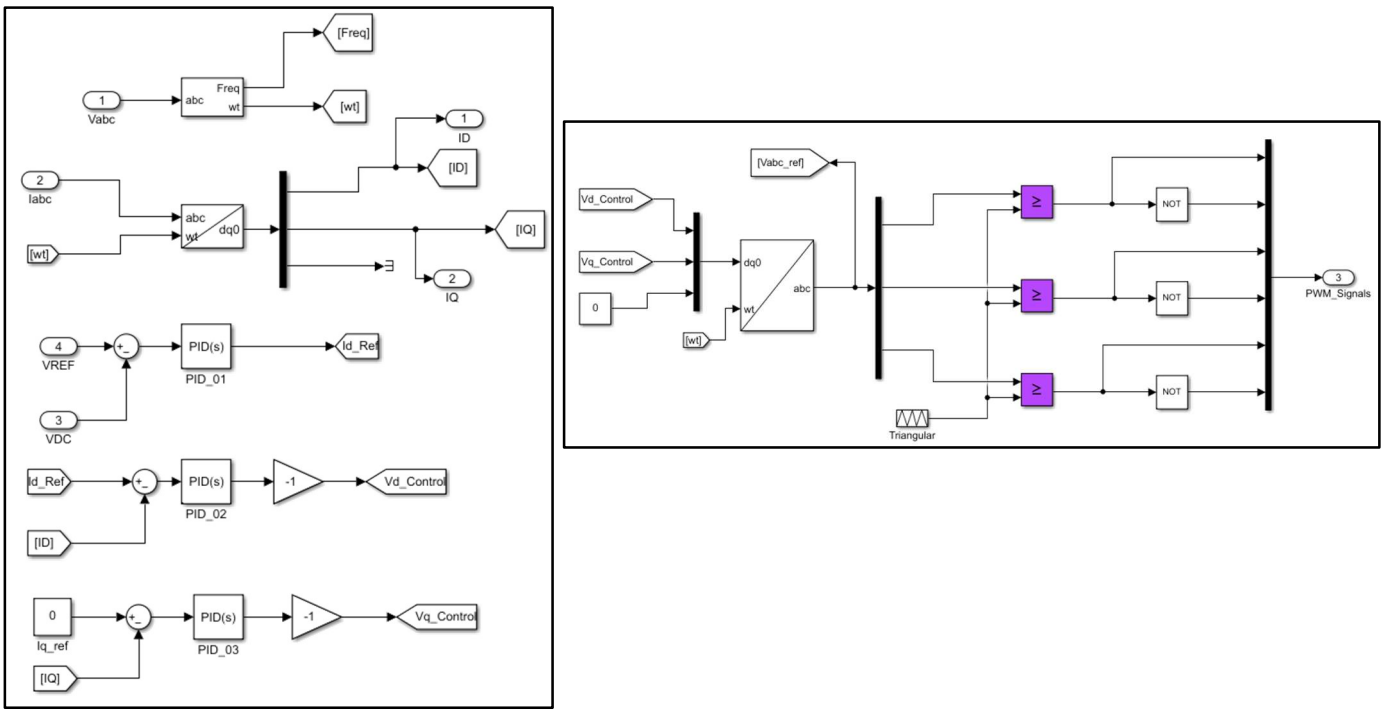

Figure: Rectifier control blocks. Park's transformation and PI controller (Left). PWM generation (Right).